Speckle Interferometry of WDS 14489+0557 and WDS 18146+0011 Binary Star Systems

Anisha Bajaj[1], Dhruv Mehrotra[2], Louis William Petersen[1], Pat Boyce[3], Mark Harris[4], Dinesh Shetty[5], Chandru Narayan[1]

[1]The Bush School, Seattle, Washington; anishabajaj10@gmail.com

[2]Redmond High School, Redmond, Washington

[3]Boyce Research Initiatives and Education Foundation (BRIEF), San Diego, CA

[4]Oorsprong Science, Roswell, Georgia

[5]Ferris State University, Big Rapids, MI

Abstract

This study investigates whether new speckle interferometry measurements of angular separation (Sep) and position angle (PA) for WDS 14489+0557 and WDS 18146+0011 are consistent with their published orbital solutions, and whether the newer Grade 4 orbit for WDS 18146+0011 may require future refinement. Observations were collected at BARON Observatory and the Mount Wilson 60-inch telescope, then processed using bispectrum analysis to measure Sep and PA. The results were compared with published ephemerides from the Washington Double Star Catalog (WDS). The measurements yielded a mean Sep and PA of $1.08'' \pm 0.02''$ and $275.77^{\circ} \pm 0.88^{\circ}$, respectively, for WDS 14489+0557, and a mean Sep and PA of $1.40'' \pm 0.02''$ and $93.60^{\circ} \pm 0.99^{\circ}$, for WDS 18146+0011. The measurement for WDS 14489+0557 is consistent with the ephemeris published in the WDS. However, the measured separation for WDS 18146+0011 differs from the published ephemeris, suggesting that the current orbital solution may benefit from further refinement.

1 Introduction

Visual binary stars provide an important way to test and refine stellar orbits because repeated measurements of angular separation (Sep) and position angle (PA) can be compared with published orbital solutions. In visual binary studies, observers measure the apparent orbit of the secondary star relative to the primary star. This apparent orbit is the projection of the true orbit onto the plane of the sky and is described through repeated Sep and PA measurements over time.

To support that these systems are physically associated rather than optical doubles, Gaia Data Release 3 (DR3) parallaxes and proper motions were used (Gaia Collaboration et al. 2023). The parallax uncertainties were then evaluated using the Distance Probability Calculator developed by Bob Buchheim and Pat Boyce, which estimates the probability that the two components are within 1.0 light-year of each other. As shown in Table 1, both systems have high probabilities of physical association, supporting their use as visual binary targets in this study.

Table 1. Gaia DR3 Astrometry, Kinematics, and Physical Association.

Parameter	WDS 14489+0557 (A)	WDS 14489+0557 (B)	WDS 18146+0011 (A)	WDS 18146+0011 (B)
Spectral Type	F6V	F8V	F2	F5
Parallax (mas)	16.172±0.043	16.158±0.048	11.922±0.025	11.919±0.023
PM RA (mas/yr)	-55.12	-54.98	15.77	15.81
PM Dec (mas/yr)	-32.41	-32.35	-24.09	-24.05
Buchheim Prob. (< 1 ly)	98.4%		99.1%	

WDS 14489+0557 was selected because it is categorized as a Grade 2 orbit in the Sixth Catalog of Orbits of Visual Binary Stars (Hartkopf et al. 2001), with the currently published orbit determined by Izmailov et al. (2019). Since its orbital elements are relatively well constrained, this system serves as a comparison target for testing whether our measurement process agrees with a reliable published orbit.

WDS 18146+0011 was selected because it is categorized as a Grade 4 orbit in the Sixth Catalog of Orbits of Visual Binary Stars (Hartkopf et al. 2001), with the current orbit determined by Scardia et al. (2015). Because Grade 4 orbits are less certain than Grade 2 orbits, this system is more likely to benefit from future revision. Several measurements have been made for this system, including a later speckle measurement by Mason and Hartkopf (2017), which reported a separation larger than the Scardia et al. (2015) ephemeris. Because its orbital elements are less well constrained, WDS 18146+0011 is a useful target for evaluating whether continued high-resolution observations may support future refinement of the published orbit. The specifications of both systems are given in Table 2, including their constellations, distances, orbital periods, component magnitudes, and orbit grades.

Table 2. Specifications of the binary stars studied in this work.

Property	WDS 14489+0557	WDS 18146+0011
Constellation	Virgo	Serpens
Distance (light-years)	202	274
Period (yr.)	225.51	344.84
Magnitude (primary)	7.02	8.22
Magnitude (secondary)	8.95	8.55
Grading	Grade 2	Grade 4

The objective of this study is to determine whether speckle interferometry measurements obtained at BARON Observatory and the Mount Wilson 60-inch telescope are consistent with the published orbital solutions for WDS 14489+0557 and WDS 18146+0011. A second goal is to evaluate whether the less certain Grade 4 orbit for WDS 18146+0011 may benefit from additional refinement. The published orbital solutions and ephemerides used for comparison were taken from the Washington Double Star Catalog and the Sixth Catalog of Orbits of Visual Binary Stars (Mason et al. 2001; Hartkopf et al. 2001).

This paper is organized as follows. Section 2 describes the equipment and methods used to carry out the observations. Section 3 presents the measured Sep and PA values. Section 4 discusses the comparison between the measured values and the published ephemerides, including the possible refinement of the orbit for WDS 18146+0011. Section 5 summarizes the conclusions.

2 Equipment and Methods

This research was made possible by the Boyce Research Initiatives and Education Foundation (BRIEF) (Boyce Research Initiatives and Education Foundation 2024). The observations were obtained using the 17-inch PlaneWave CDK telescope located at the BARON Observatory at Sierra Remote Observatory near Auberry, California, operated by BRIEF. The telescope was configured with a 2.5× TeleVue Powermate, increasing the effective focal length to 7348 mm and changing the effective focal ratio to f/16.8. Additional observations were obtained using the 60-inch reflector telescope located at the Mount Wilson Observatory (MWO) in California, which belongs to the Mount Wilson observatory. The large aperture, long focal length, and precise tracking of both telescopes enable high-resolution observations of close binary systems. In practice, this setup allowed separations of approximately 0.8 arcsec for BARON and 0.5 arcsec for MWO to be measured under the observing conditions used in this study. These values should be understood as practical observing limits rather than theoretical diffraction limits, which are smaller and depend primarily on telescope aperture and observing wavelength. A more complete description of the equipment used is provided in Table 3.

Table 3. Equipment Specifications.

Observatory	Scope Aperture	Focal Length / F-Ratio	Camera Used	Resolution (arcsec/pixel)
Mount Wilson Observatory (MWO)	60 inches	24,000 mm (f/16)	ZWO ASI 6200MM Pro	0.0306
Boyce Astro Research Observatory North (BARON)	17 inches	7,348 mm (f/16.8)	ZWO1600M	0.106

The images from both telescopes were processed using speckle interferometry, which requires a large number of high-resolution images to remove atmospheric distortion and other unwanted interference. This is a high-resolution imaging technique that is used to overcome the blurring effects of atmospheric turbulence, which can severely limit the resolution of ground-based telescopes. In this method, many short-exposure images (typically on the order of milliseconds) are taken to record the random speckle patterns caused by atmospheric distortion. By performing bispectrum analysis these patterns can be analyzed to extract the true high-resolution information about the observed object, such as the Sep, PA, and magnitude difference between binary star components.

The raw images were processed using the Speckle Toolbox software developed by Harshaw et al. (2017). It is an integrated package designed for handling short-exposure image stacks. The software compiled 500 images from BARON into a Flexible Image Transport System (FITS) cube and 1000 images from MWO into a separate FITS cube (Pence et al. 2010). This results in a multidimensional file format that preserves critical spatial and temporal details for high-precision measurement and image reconstruction. The software then applied bispectrum phase analysis to reconstruct the binary system image, isolate the position of the companion star relative to the primary, and refine the extracted binary parameters: separation (ρ) and position angle (Θ).

To reduce the effects of sky conditions and observer-to-observer variation, the measurements for each system were averaged across different nights, both telescope systems (BARON and MWO), and multiple observers. After compiling the data, anomalous measurements were removed using an interquartile range (IQR) method, where values that fell outside the central range of the dataset were identified as outliers and excluded. Since the remaining measurements came from two different telescope systems, small differences between the systems may have affected the final uncertainties. This is especially important for the position angle (Θ), where the standard deviations were 0.88° for WDS 14489+0557 and 0.99° for WDS 18146+0011. These uncertainties may have been caused by seeing conditions, signal-to-noise limits, small differences in aperture placement, and differences between observers. Therefore, the reported uncertainty reflects both the variation between repeated measurements and possible small differences between the two telescope systems.

Figure 1 shows an example of speckle interferometry showing the primary and secondary stars resolved for the binary system WDS 14489+0557. The image on the left is the unresolved image, and the image on the right is the resolved image.

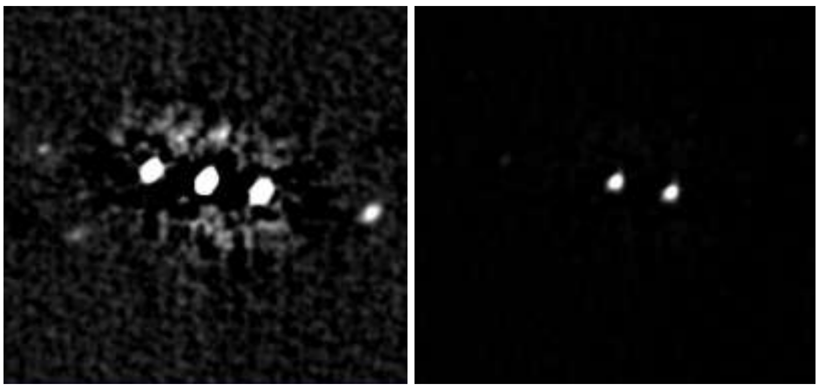

Figure 1: The unresolved speckle image (left) and resolved image (right) for WDS 14489+0557

Figure 2 shows an example of the bispectrum analysis for the binary system WDS 14489+0557. The star on the left is the primary star and the one on the right is the secondary star.

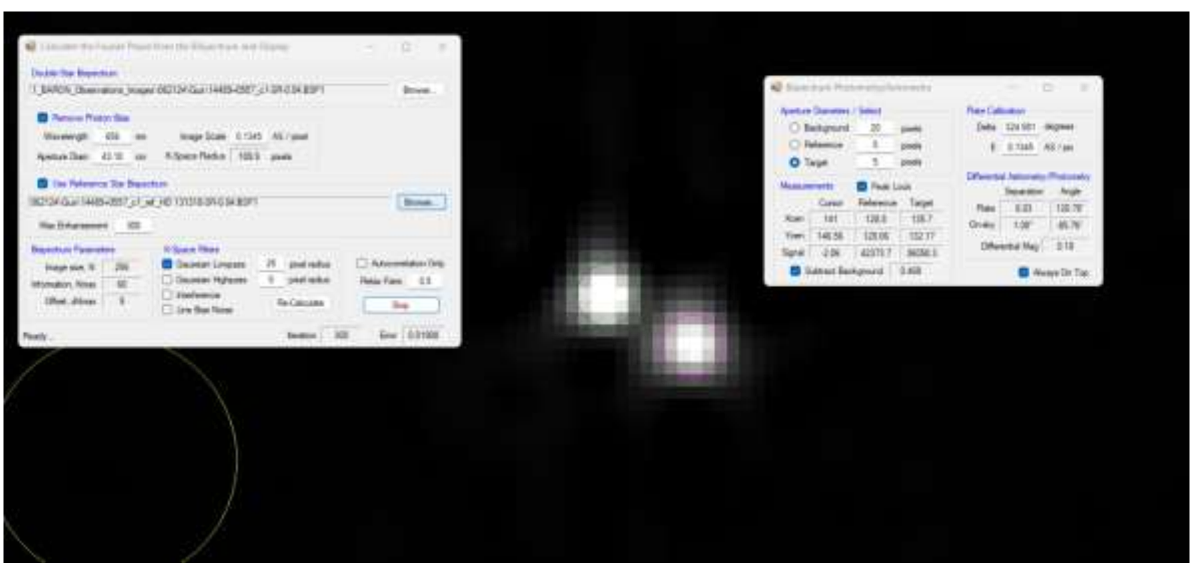

Figure 2: Screenshot of the data reduction on WDS 14489+0557

Figure 3 below shows an example of speckle interferometry showing the primary and secondary stars resolved for the binary system WDS 18146+0011. The figure on the left is the unresolved image, and the figure on the right is the resolved image.

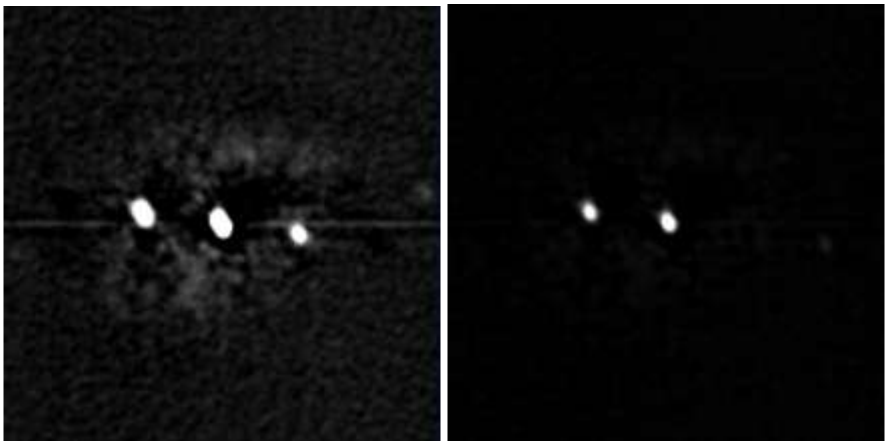

Figure 3: The unresolved speckle image (left) and resolved image (right) for WDS 18146+0011

Figure 4 shows an example of the bispectrum analysis for the binary system WDS 18146+0011. The star on the right is the primary star and the one on the left is the secondary star.

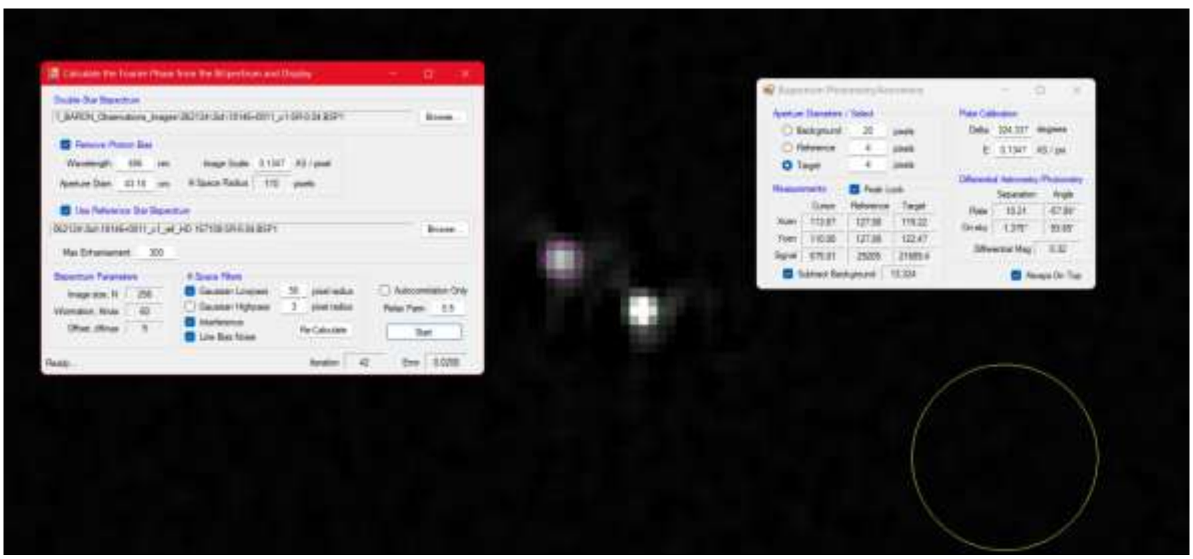

Figure 4: Screenshot of the data reduction on WDS 18146+0011

3 Data

Data were collected over two nights (June 21 and June 27, 2024) for WDS 14489+0557 and 18146+0011 as shown in Table 4 and Table 5, respectively. The reference stars chosen were HD 131318 and HD 167108, respectively.

The data were analyzed using the speckle reduction technique described in Section 2. The average results are shown in Table 6 and Table 7. Mean and standard deviation values are rounded for reporting, while Standard Error of the Mean (SEM) and Z-scores were calculated from the unrounded measurements.

Table 4. Data collected for WDS 14489+0557.

WDS 14489+0557							
Reference Star: HD 131318 (BARON), M5 (MWO)			Discoverer: STF1883				
Date	Epoch	Observatory	Exposure (msec)	Filter	Images per cycle	Number of cycles	Star (S) /Reference (R)
06/21/2024	2024.470	BARON	40	Sloan r 656nm	500	1	S
06/21/2024	2024.470	BARON	40	Sloan r 656nm	500	1	R
06/27/2024	2024.486	MWO	50	Sloan r 629nm	1000	1	S
06/27/2024	2024.486	MWO	50	Sloan r 629nm	300	1	R

Table 5. Data collected for WDS 18146+0011.

WDS 18146+0011							
Reference Star: HD 167108 (BARON), M5 (MWO)			Discoverer: STF2294				
Date	Epoch	Observatory	Exposure (msec)	Filter	Images per cycle	Number of cycles	Star (S) /Reference (R)
06/21/2024	2024.470	BARON	40	Sloan r 656nm	500	1	S
06/21/2024	2024.470	BARON	40	Sloan r 656nm	500	1	R
06/27/2024	2024.486	MWO	50	Sloan r 629nm	1000	1	S
06/27/2024	2024.486	MWO	50	Sloan r 629nm	300	1	R

Table 6. Measured mean position angle (θ) and angular separation (ρ) for WDS 14489+0557.

WDS 14489+0557				
Epoch	Measurement	Theta (θ) deg	Rho (ρ) arcsec	Delta Magnitude
2024.470 2024.486	Mean	275.77	1.08	0.25
	Standard Deviation	0.88	0.02	0.0793
	Standard Error of the Mean	0.265	0.0051	0.0239
Ephemeris		276.5	1.066	
Z-score		-2.75	2.75	

Table 7. Measured mean position angle (θ) and angular separation (ρ) for WDS 18146+0011.

WDS 18146+0011				
Epoch	Measurement	Theta (θ) deg	Rho (ρ) arcsec	Delta Magnitude
2024.470 2024.486	Mean	93.60	1.40	0.52
	Standard Deviation	0.99	0.02	0.1227
	Standard Error of the Mean	0.298	0.0048	0.0370
Ephemeris		93.1	1.3470	
Z-score		1.68	11.04	

4 Discussion

The Z-scores in Tables 6 and 7 quantify how far each measured mean differs from the published ephemeris relative to the standard error of the mean. They were calculated using the following equation.

$$Z = \frac{\bar{x} - x_{\text{ephem}}}{\text{SEM}} \qquad (1)$$

where $\bar{x}$ is the measured mean, x_{ephem} is the published ephemeris value, and SEM is the standard error of the mean.

For WDS 14489+0557 (Grade 2), the Z-score for PA is -2.75 and the Z-score for Sep is 2.75. Because both values fall within the adopted ±3 uncertainty boundary, the measurements are consistent with the published ephemeris, so a new orbital model is not supported by these data. For WDS 18146+0011 (Grade 4), the Z-score for PA is 1.68, but the Z-score for Sep is 11.04. This separation value falls outside the adopted uncertainty boundary and suggests that the published orbit may benefit from further refinement. However, since this interpretation is based on one recent measurement point with non-negligible uncertainty, it should be treated as evidence for a possible orbit refinement rather than confirmation of a new orbit.

To further investigate this deviation, the observations were analyzed using the Speckle Toolbox (STB) orbit optimization feature. To establish a baseline for comparison, the orbital solution was first computed using the STB with equal weights (w = 1) assigned to all measurements, regardless of observational technique. This represents an unbiased fit where each data point contributes equally to the model. The STB optimizer adjusts the orbital parameters to minimize the weighted root mean square deviation (WRMSD) between observed and computed positions. The WRMSD from this initial fit serves as a reference point for evaluating the impact of the weighting scheme applied in the next step.

Figure 5 shows the initial STB orbital fit with equal weights applied to all measurements. The corresponding WRMSD for this fit was 48.59, which reflects the overall deviation between the observed data and the model when all measurements are treated equally.

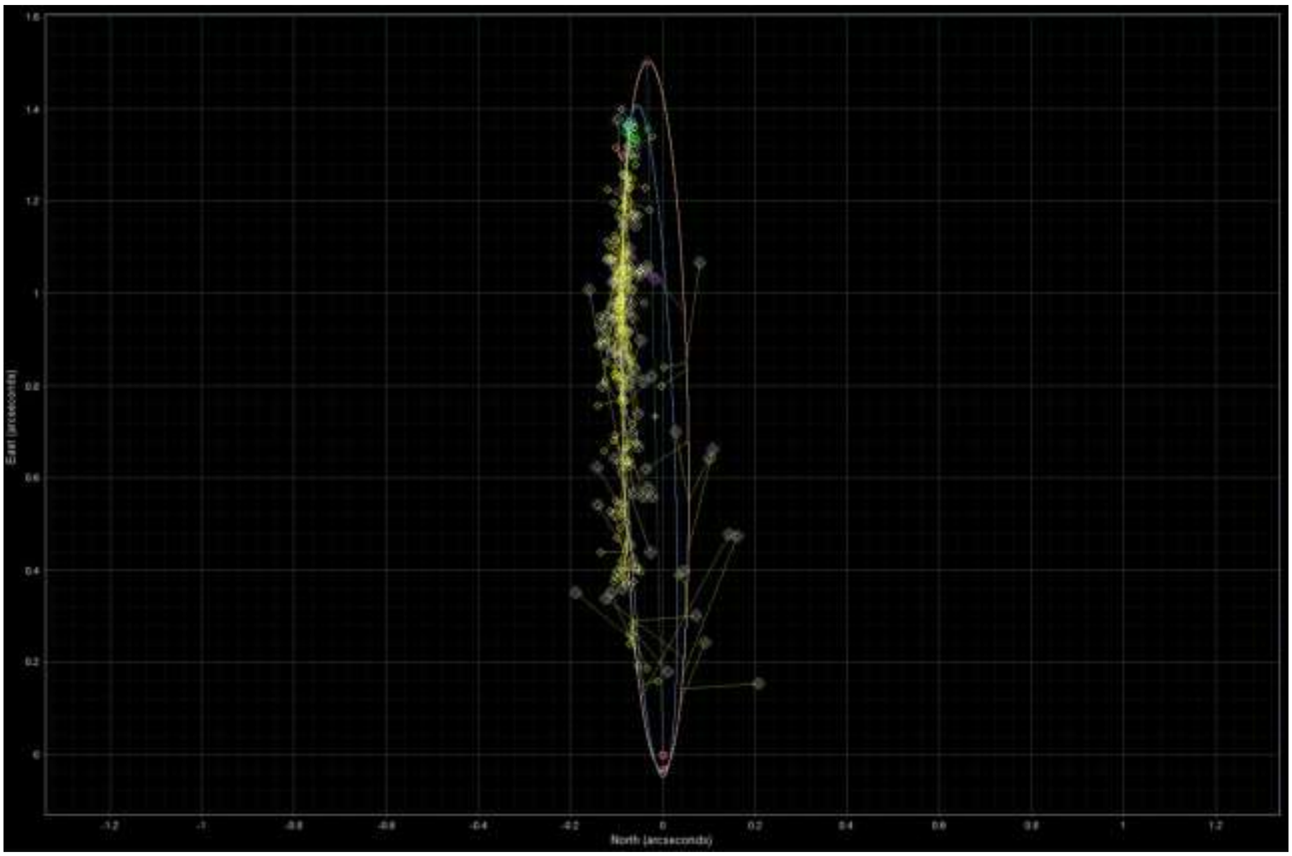

Figure 5: Initial orbital fit for WDS 18146+0011 generated using the Speckle Toolbox with equal weights (w = 1) applied to all measurements. The WRMSD for this fit is 48.59.

Following this baseline solution, a weighted optimization was performed. Because measurements of visual binaries are obtained using a variety of observational methods with different levels of accuracy, each observation was assigned a weight based on its measurement technique. The weights used in this analysis were inferred from the weighting hierarchy described by Hartkopf et al. (2001), which gives relative guidance for the expected precision of different observational methods. These values should not be interpreted as fixed standard weights. Because the STB optimizer allows only a limited number of technique codes, the original technique codes were grouped into broader categories. The final weights for each group were then calculated using a weighted mean based on both the original weights and the number of observations in each category:

$$\mu_w = \frac{\sum_{i=1}^{n} w_i N_i}{\sum_{i=1}^{n} N_i} \qquad (2)$$

where μ_w is the grouped technique-code weight, w_i is the original technique-code weight, N_i is the number of observations assigned to that technique code, and n is the number of technique codes included in the grouped category.

Table 8 lists the original technique codes, grouped technique codes, and weights used in the orbit optimization.

Table 8. Original and Grouped Technique Codes and Weights for WDS 18146+0011.

WDS 18146+0011					
Original Technique Code	Description	Weight	Number of Data Points for each Technique Code	New Grouped Technique Code[1]	New Code Weight
Mb	Refractor Micrometry	0.2	7	M	0.133
Ma	Early Micrometry	0.05	178		
Mc	Calibrated Micrometry	0.4	4		
Mr	Transit Circle	0.05	1		
Su[2]	Survey Data	0.8	20		
Cl	High-Resolution CCD	2	3	C	1.70
Cu	Conventional CCD	1	1		
Ce	Early Electronic CCD	0.7	1		
Ca	Coronagraphic Imaging	2.5	1		
S	Speckle Interferometry	10	413	S	10.034
St	Speckle w/ Triple Correlation	15	2		
Se	Speckle (Epochal)	12	2		
Ht	Hubble Space Telescope	50	2	Ht	50
Hh	Hipparcos Original	65	3	Hh	65
Hg	HTS Sensor Interferometry	4	4	Hg	4
Zp	Zone Photographic Plate	0.1	1	Zp	0.1

[1]Arbitrary group designations created for this study due to software limitations.

[2]Su was grouped under M because this category includes techniques with weights below 1.

The application of the weighted optimization reduced the WRMSD from 48.59 to 21.70, suggesting that the weighting scheme produced a better fit for this dataset. However, this should not be interpreted as confirmation of a replacement orbit. The effect of this optimized fit is shown in Figure 6.

Figure 6 shows the binary system WDS 18146+0011, in which the blue ellipse is the optimized orbit calculated in this work and the orange ellipse is the currently published orbit. The *MWO2024* point represents the measurement from the present work. The other points shown are previous observations from the Sixth Orbit Catalog. The highlighted points were removed from the optimization because they differed from the published orbit by more than 70 mas. This cutoff was chosen because a 70 mas difference is greater than three standard deviations from the main group of measurements. These points were therefore treated as outliers, since they were likely affected by measurement uncertainty or poor observational conditions.

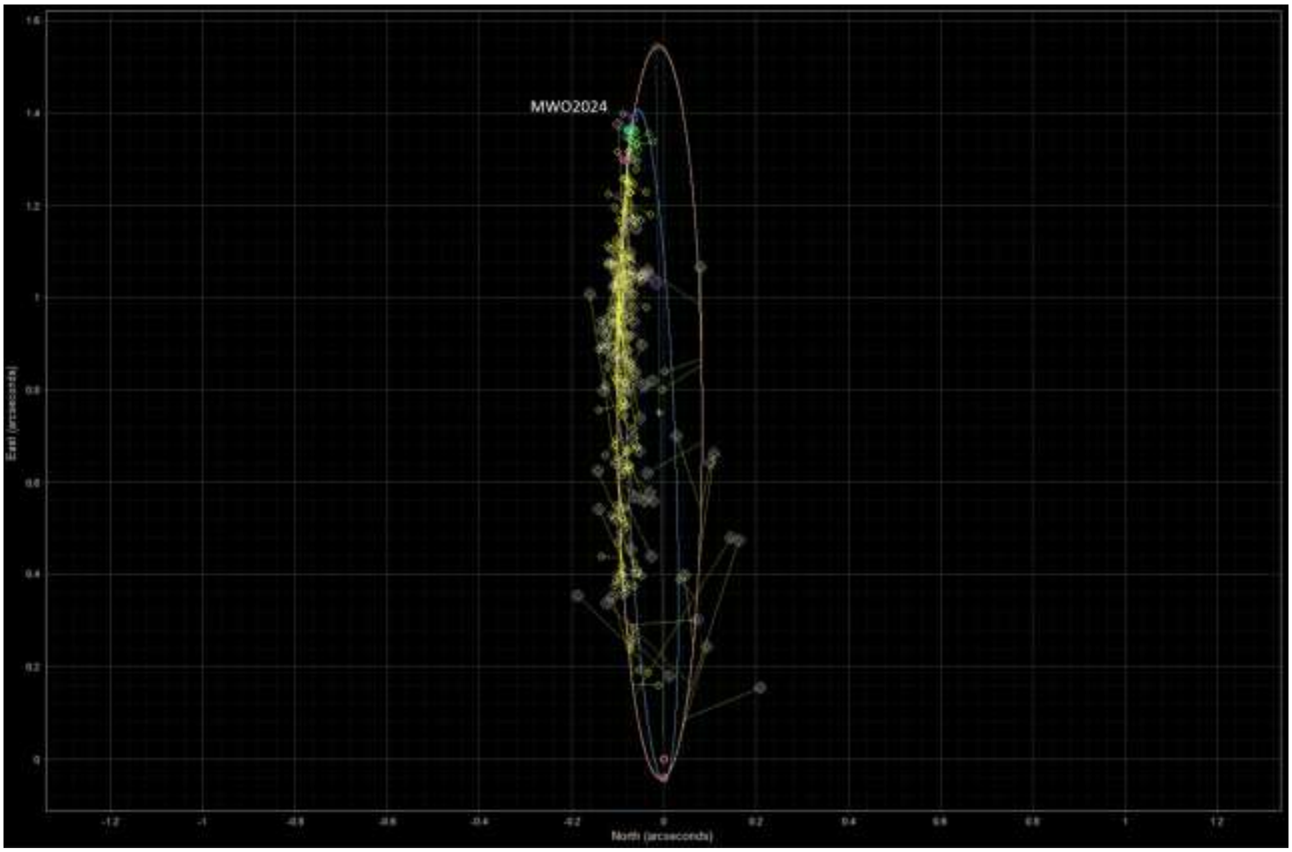

Figure 6: Apparent orbital plot of WDS 18146+0011 with historical data from the Sixth Orbit Catalog. The white diamond point (MWO2024) is the observation from the present work. The plot shows the published orbit and the optimized orbit calculated in this work after orbital optimization

The orbital elements in Table 9 provide the main comparison between the published orbit and the optimized orbital solution. This optimized solution is consistent with a longer orbital period and a modest increase in eccentricity relative to the published orbit. The MWO2024 observation was assigned a weight of 12 under the weighting scheme used in this study because it represents the new high-precision speckle measurement from the observing epoch. This allowed the MWO2024 point to carry somewhat greater influence in the optimized fit than the broader speckle category 'S' listed in Table 8, but this effect should be interpreted cautiously because the measurement has non-negligible uncertainty.

The revised orbital elements suggest a possible refinement to the published orbit for WDS 18146+0011, but they do not confirm a replacement orbit. Most of the historical observations are concentrated along a limited portion of the apparent orbit, so the orbital elements remain weakly constrained. Additional high-precision observations over future epochs are needed to determine whether the longer-period solution remains stable.

Table 9. Orbital Elements for WDS 18146+0011 from the Sixth Orbit Catalog and the Optimized Orbit calculated in this work.

Orbital Parameters	Published Orbital Elements	Optimized Orbital Elements
Period (yrs)	344.84	413.81
Semi-major axis (arcsec)	0.732	0.8121
Eccentricity	0.935	0.9484
Inclination (deg)	101.6	110.37
Long. of Asc. Node (deg)	91.1	85.9
Time at Periastron (year)	1890.086	1888.753
Long. of Periastron (deg)	173.8	166.54

5 Conclusions

This study compared new speckle interferometry measurements of WDS 14489+0557 and WDS 18146+0011 with their published orbital solutions. The measurements for WDS 14489+0557 are consistent with the ephemeris from the published orbit in the Sixth Catalog of Visual Binary Stars, supporting the reliability of the measurement process. For WDS 18146+0011, the separation Z-score of 11.04 falls outside the adopted ±3 uncertainty boundary, suggesting that the published orbit may benefit from further refinement. The optimized orbital solution is consistent with a longer orbital period and a modest increase in eccentricity. However, because this interpretation is based on one recent measurement point, it should be considered preliminary until additional high-precision observations are available.

Acknowledgements

This research made use of the Washington Double Star Catalog, maintained at the U.S. Naval Observatory, as well as data from the European Space Agency's Gaia mission, processed by the Gaia Data Processing and Analysis Consortium. The observations used in this paper were collected at BARON Observatory using the 17-inch PlaneWave CDK telescope and at Mount Wilson Observatory using the 60-inch telescope. We are grateful to the Boyce Research Initiatives and Education Foundation (BRIEF) for their support. We would also like to thank Bob Buchheim for providing his radial-distance probability method, David Rowe for authoring Speckle Toolbox, and August Kotovic for assistance with processing.

References

Boyce Research Initiatives and Education Foundation. "BRIEF." Boyce-Astro, 2024, www.boyce-astro.org.

Gaia Collaboration, Vallenari, A., Brown, A. G. A., Prusti, T., de Bruijne, J. H. J., Arenou, F., Babusiaux, C., Biermann, M., Creevey, O. L., Ducourant, C., et al. 2023. Gaia Data Release 3: Summary of the content and survey properties. *Astronomy & Astrophysics*, 674:A1.

Harshaw, R., Rowe, D., and Genet, R. 2017. The Speckle Toolbox: A Powerful Data Reduction Tool for CCD Astrometry. *Journal of Double Star Observations*, 13(1):52.

Hartkopf, W. I., Mason, B. D., and Worley, C. E. 2001. The 2001 US Naval Observatory Double Star CD-ROM. II. The Fifth Catalog of Orbits of Visual Binary Stars. *The Astronomical Journal*, 122(6):3472–3479.

Izmailov, I. S. 2019. The orbits of 451 wide visual double stars. *Pisma v Astronomicheskii Zhurnal*.

Mason, B. D., Wycoff, G. L., Hartkopf, W. I., Douglass, G. G., and Worley, C. E. 2001. The 2001 US Naval Observatory Double Star CD-ROM. I. The Washington Double Star Catalog. *The Astronomical Journal*, 122(6):3466–3471.

Mason, B. D., and Hartkopf, W. I. 2017. Speckle Interferometry at the U.S. Naval Observatory. XXII. *The Astronomical Journal*, 154(5), 183.

Pence, W. D., Chiappetti, L., Page, C. G., Shaw, R. A., and Stobie, E. 2010. Definition of the Flexible Image Transport System (FITS), version 3.0. *Astronomy & Astrophysics*, 524, A42.

Scardia, M., Prieur, J.-L., Pansecchi, L., and Aristidi, E. 2015. Speckle observations with PISCO in Merate, Italy: XIV. Astrometric measurements of visual binaries in 2013 and new orbits for ADS 1097, 5871, 7203, 7775, 9378, 9578, and 11186. *Astronomische Nachrichten*.